

Photochromism and Thermochromism of Spiro[indolinoxazines] in Normal and Reversed Micelles

Gianna Favaro* and Fausto Ortica

Dipartimento di Chimica, Università di Perugia, 06123 Perugia, Italy

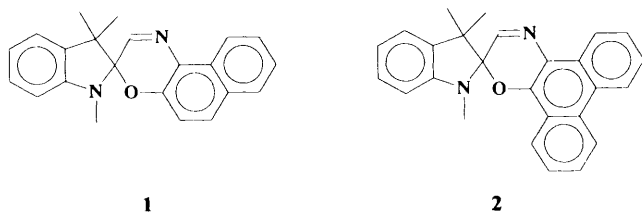
Vincenzo Malatesta

Great Lakes Chemical Italia S.r.l., 20097 San Donato Milanese, Italy

Spectra, photochromism and thermochromism of a spiro[indoline-naphthoxazine] and a spiro[indoline-phenanthroxazine] have been investigated in cationic (CTAB, hexadecyltrimethylammonium bromide) and non-ionic (TX-100) micellar solutions and in sodium bis-2-ethylhexylsulfosuccinate (AOT)/toluene/water inverted-micelles. The spectral shifts of the photomerocyanine colour band provided information on the location of the molecules in these systems. From photokinetic study of the colour-forming and colour-fading reactions, the quantum yield and bleaching constant were determined. The thermal equilibrium constant of the spiro[indoline-phenanthroxazine] was spectrophotometrically measured. Comparison of the results obtained in microheterogeneous systems with those determined in a homogeneous solution indicated that thermo- and photo-colourability increase in TX-100 and CTAB micelles and decrease in inverted micelles.

Studies on photochromism of spiropyrans and spirooxazines have been carried out in various organic solvents as well as in different media, such as polymer matrix,¹ liposomal membranes,² monolayers³ and bilayer-clay matrices.⁴ Only a few studies have been carried out in micelles.⁵ Photochromic molecules solubilised in micelles have been suggested as probes for the study of the hydrodynamics of fluids.⁶

The molecules studied here are 1,3,3-trimethylspiro[indoline-2,3'-[3H]naphth[2,1-b][1,4]oxazine], **1**, and spiro[indoline-2,2'-[2H]phenanthr[9,10-b][1,4]oxazine], **2**, the behaviour of which was previously investigated in organic solvents.^{7–9}



The photochromism of these molecules is due to photocleavage of the C–O spirobond of the spirooxazine (SO) upon UV irradiation, which gives the open photomerocyanine structure (PM) which absorbs in the visible region. The reaction is thermoreversible; in the dark, the photoproduct merocyanine reconverts to SO within a few seconds. These compounds, which are wholly insoluble in water, can be solubilised in micellar aqueous solution. Inclusion in a micelle can produce changes in the chromatic properties, as well as in the photokinetic behaviour; thermal- and/or photo-reactions can occur over different timescales and the photo-products may be forced to assume preferred conformations. Charged interfaces can strongly influence reactions involving polar or ionic reactants and products. Moreover, the shielding role of the micellar surface can increase the durability of these photochromic systems.

In this paper, the micellar effects on the absorption spectrum of the coloured PM and the thermodynamic and photokinetic characteristics of the colour-forming reversible reaction were investigated in TX-100 and CTAB micellar aqueous solution, as well as in reversed AOT micelles which have a highly organised hydrophilic/hydrophobic interface.

The results are compared with those obtained in homogeneous solutions.

Experimental

Materials

1 and **2** were prepared according to literature methods.⁹ The surfactants, hexadecyltrimethylammonium bromide (CTAB) (BDH, specially pure), TritonX-100 (TX-100) (Fluka) and aerosol-OT (sodium bis-2-ethyl-hexylsulfosuccinate, AOT) (Fluka) were used as supplied. Values of the critical micellar concentration, c.m.c., for CTAB ($9.2 \times 10^{-4} \text{ mol dm}^{-3}$) and TX-100 ($2.6 \times 10^{-4} \text{ mol dm}^{-3}$) and aggregation numbers, *N*(60 and 143 for CTAB and TX-100, respectively) were taken from the literature.¹⁰ AOT reversed micelles were obtained by adding definite amounts of water (0.2, 0.4, 0.5, 0.8 mol dm⁻³) to a 0.1 mol dm⁻³ AOT solution in toluene (RS Carlo Erba), following a literature procedure.¹¹

For comparing results in microheterogeneous and homogeneous media and investigating viscosity effect, linear chain alcohols, methanol (Fluka), ethanol (RS, Carlo Erba), propanol (Fluka), pentanol (Fluka) and octanol (Fluka), were used without further purification.

All experiments were performed using freshly prepared solutions; macroscopic homogeneity was obtained by sonication.

Equipment

Absorption spectra were recorded on a Perkin-Elmer Lambda 5 or a Perkin-Elmer Lambda 16 spectrophotometer. A cryostat (Oxford Instruments) was used for the temperature control. A 250 W medium-pressure mercury lamp, filtered by an interference filter ($\lambda = 366 \text{ nm}$), was used for producing the coloured PM form.

Corrected emission spectra were recorded using a Spex Fluorolog-2 FL 112 spectrofluorimeter.

Measurement conditions

Emission Measurements

To measure the emission quantum yields, Φ_F , corrected areas of a standard compound (quinine sulfate in 1 mol dm⁻³ H₂SO₄, $\Phi_F = 0.546$)¹² and the sample $\{[SO] = (1-$

$1.5) \times 10^{-5} \text{ mol dm}^{-3}$; $A_{\text{SO}} = 0.05\text{--}0.1$ emissions were compared and corrected for the refractive index of the medium.

Thermo-equilibrium Measurements

To observe the thermal equilibrium, the initial concentration of SO was kept as high as possible $[(4\text{--}6) \times 10^{-5} \text{ mol dm}^{-3}]$. The solutions were spectrophotometrically analysed in the visible absorption region of the open PM form. The absorptions were taken with the surfactant in the reference cell.

Photokinetic Measurements

Micellar solutions were prepared so as not to have an occupancy number larger than unity, in order to ensure a preferential mono-occupancy, on the basis of a Poisson distribution. The concentrations of the starting SO were of the order of $(2\text{--}5) \times 10^{-5} \text{ mol dm}^{-3}$, corresponding to absorbances in the range 0.1–0.3 at the irradiation wavelength (366 nm). This wavelength was not absorbed by the surfactants. Exposure of the sample (cell: 1 cm path length, 1 cm³ solution) to light was carried out in the spectrophotometer cell at 90° to the analysis light. The increase of the PM absorbance, under stationary irradiation and constant temperature, was followed at the absorption-maximum wavelength (565–616 nm), where the excitation light did not disturb the absorbance measurement, up to photostationary state attainment. The irradiation intensity, which was constant during each run, was determined using potassium ferrioxalate actinometry (typically, $10^{-6} \text{ Einstein dm}^{-2} \text{ s}^{-1}$).

The kinetic rate parameters of the ring-closure reaction were determined by following the disappearance of the coloured form at the wavelength of maximum absorbance, after having removed the irradiating source. First-order rate constants were obtained from linear log *A* vs. time plots (correlation coefficient >0.99, using *ca.* 100 experimental points); the reproducibility over different solutions was within 10%. The activation energy of the thermal back reaction was determined from Arrhenius plots: an uncertainty of *ca.* 10% was evaluated for the homogeneous solutions, while the estimated uncertainty was greater (*ca.* 20%) for the heterogeneous solutions, owing to the restricted temperature range used (280–300 K) in order not to affect the micellar structure.¹³ The frequency factors, obtained by extrapolation from Arrhenius plots over a limited experimental temperature range, were affected by a greater error (>50%).

Results

Absorption and Emission Spectra

The absorption spectra of the two photochromes under study were taken in microheterogeneous solutions of direct (TX-100 and CTAB) and inverted (AOT/toluene/water) micelles, after having produced the open PM form by UV irradiation. In Table 1, the absorption maxima measured are compared with those in ethanol, toluene and methylcyclohexane. The spectra of the two molecules in different media are illustrated in Fig. 1. As can be seen, the band progressively shifts to the blue

Table 1 Absorption maxima (λ/nm) of **1** and **2** PMs in micellar solutions, compared with homogeneous solutions [ethanol (EtOH), toluene, methylcyclohexane (MCH)]

	CTAB	TX-100	AOT	EtOH	toluene	MCH
1	616 (54)	613 (51)	600 (38)	613	601	585
2	609 (57)	603 (53)	582 (37)	600	588	566

Interpolated $E_T(30)$ values are indicated in parentheses.

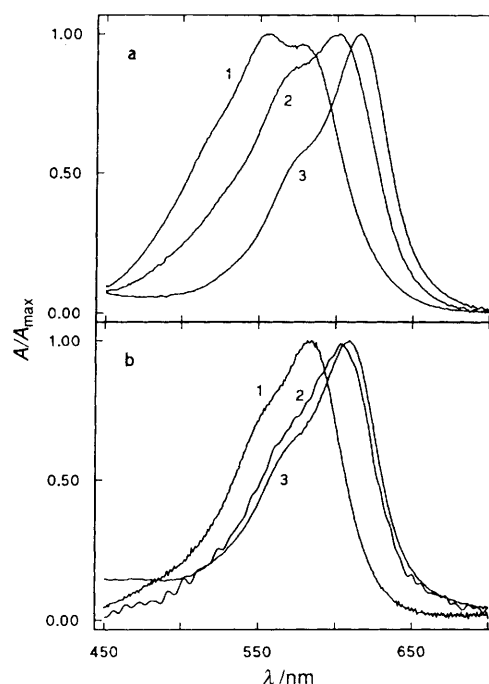


Fig. 1 Normalised absorption spectra of the PMs obtained from **1** and **2** in different media. (a) **1** in MCH (1), AOT/toluene/water (2) and CTAB (3); (b) **2** in AOT/toluene/water (1), TX-100 (2) and CTAB (3).

from CTAB to TX-100 to AOT. A change in shape of the absorption band is observed for **1**.

Fluorescence was also investigated. Generally, emissions from spiro[oxazines] have to be considered cautiously, because they are very weak (owing to efficient competition of the opening reaction) and can sometimes originate from some impurity or degradation product.¹⁴ However, in the case of **1**, the very weak emission found in ethanol ($\lambda_{\text{max}} = 422 \text{ nm}$) was assigned to the closed molecule. Thus, it seemed worthwhile to investigate the micellar effect on this emission. Fluorescence spectra and fluorescence quantum yields were measured at different occupancy numbers, n ($n = [\text{SO}]/[\text{micelle}]$) in TX-100 micellar solution, which is the most similar in polarity to ethanol. The results were compared with ethanol ($\eta = 1.08 \text{ mPa s}$) and octanol ($\eta = 7.38 \text{ mPa s}$) to obtain some indication of the viscosity effect (Table 2). As can be seen, the Φ_F decreases with increasing n in TX-100, but it is more than an order of magnitude higher than in ethanol. At high occupation number ($n = 2.14$), the Φ_F is close to the value obtained in octanol.

Photokinetics

The photokinetics of the ring-opening reactions of **1** and **2** were studied in microheterogeneous micellar systems; the results were compared with those obtained in a homogeneous solution. Temperature was rigorously controlled in order to

Table 2 Fluorescence quantum yields, Φ_F , of **1** in TX-100 micellar solution and alcohol solutions [ethanol (EtOH) and octanol (OtOH)]

	concentration/mol dm ⁻³	<i>n</i>	Φ_F
TX-100	1.71×10^{-2}	0.11	3.3×10^{-3}
	3.43×10^{-3}	0.50	1.8×10^{-3}
	9.56×10^{-4}	2.14	1.3×10^{-3}
EtOH			9.0×10^{-5}
OtOH			1.5×10^{-3}

keep the rate parameter of the thermal back reaction, k_A , constant. Assuming that the quantum yield of the reverse photoreaction is negligible, the kinetics of the colour-forming process is expressed by eqn. (1) in terms of the time-dependence of the PM absorbance (A_{PM}) at the measurement wavelength.⁸

$$\frac{dA_{PM}}{dt} = \varepsilon_{PM} \Phi_R I^0 F A'_{SO} - k_A A_{PM} \quad (1)$$

Here, ε_{PM} ($\text{dm}^3 \text{mol}^{-1} \text{cm}^{-1}$) is the molar absorption coefficient of the PM, Φ_R is the quantum yield of the photoreaction, I^0 represents the intensity of the monochromatic excitation light ($\lambda_{exc} = 366 \text{ nm}$) per unit time ($\text{Einstein dm}^{-3} \text{s}^{-1}$), A'_{SO} is the SO absorbance at λ_{exc} and $F = [1 - \exp(-2.3A')]/A'$ represents a photokinetic factor^{15,16} (A' is the total absorbance at λ_{exc}), which accounts for the variation of the absorbed fraction of the total incident light, $I = I^0[1 - \exp(-2.3A')]$, during the reaction course.

If the ε_{PM} value is known, the quantum yield can be obtained from eqn. (1), by plotting dA_{PM}/dt vs. A_{PM} and extrapolating the colour-forming rate at zero time [eqn. (2)]:

$$\Phi_R = \frac{\left(\frac{dA_{PM}}{dt}\right)_{t \rightarrow 0}}{\varepsilon_{PM} I^0 [1 - \exp(-2.3A'_{SO})]} \quad (2)$$

An example of experimental run and quantum yield extrapolation is illustrated in Fig. 2 where the colour-forming kinetics and treatment of the experimental data based on eqn. (1) and (2) are shown. Alternatively, Φ_R can also be determined using data obtained from the photostationary state, namely when $dA_{PM}/dt = 0$ [eqn. (3)]. Then, the PM absorbance reaches a limiting value (A_{PM}^∞). Superscript ∞ refer to photostationary conditions. The limiting

$$\varepsilon_{PM} \Phi_R I^0 F^\infty A'_{SO} = k_A A_{PM}^\infty \quad (3)$$

value, A_{PM}^∞ , obtained as the horizontal asymptote from the reaction time course (Fig. 2), represents a measure of the photostationary colourability of the photochrome under fixed conditions (temperature, solvent, concentration, excitation light intensity and wavelength). The bleaching rate coefficient, k_A , can be measured from a first-order kinetic treatment of the absorption decay curve obtained after switching off the irradiating source, as shown in Fig. 3 for **1** in TX-100 micellar solution.

In determining Φ_R , the most important point is to use a reliable ε_{PM} value. Two methods, based on treatment of

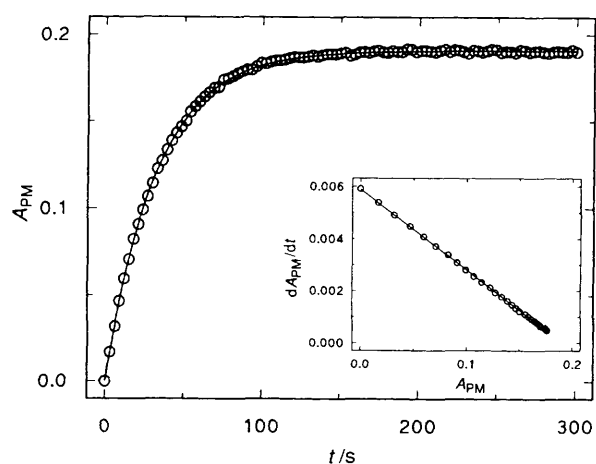


Fig. 2 Colour-forming kinetics under steady irradiation of **1** ($5 \times 10^{-5} \text{ mol dm}^{-3}$) in CTAB micellar solution. Inset: quantum-yield extrapolation based on eqn. (2).

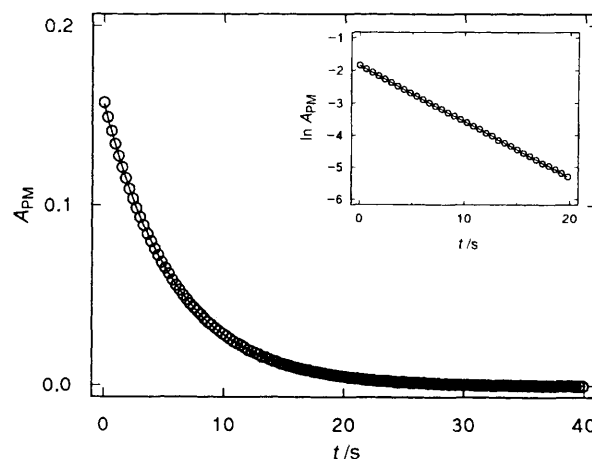


Fig. 3 Colour-bleaching kinetics of **1** in TX-100 micellar solution. Inset: first-order kinetic treatment.

spectrophotometric data, have been devised to solve this problem.^{8,16} Two different types of data sets are needed: for the first method, (a), limiting absorbances and bleaching rate parameters recorded at different temperatures; for the second method, (b), absorbance/time values measured at constant temperature. Method (a) cannot be applied in the present case, since a sufficiently large temperature range cannot be explored without changing the micellar structure. Method (b) requires relatively low bleaching rates ($k_A \leq 10^{-2} \text{ s}^{-1}$), which could be achieved by lowering the temperature; but this is impossible in a water-containing system. Thus, considering the spectral behaviour of the PMs in microheterogeneous systems, an acceptable approximation was to use the ε_{PM} values previously determined⁸ in a polar solvent (ethanol), for TX-100 and CTAB micellar solutions, and those determined in a non-polar solvent (methylcyclohexane) for AOT/benzene/water solutions. Thus, to calculate Φ_R , $\varepsilon_{PM} = 61\,000$ and $38\,000 \text{ dm}^3 \text{mol}^{-1} \text{cm}^{-1}$ were used in direct and inverted micelles, respectively, for **1**, and $\varepsilon_{PM} = 87\,000$ and $51\,000 \text{ dm}^3 \text{mol}^{-1} \text{cm}^{-1}$ in direct and inverted micelles, respectively, for **2**.

The results of the photokinetic study (k_A and Φ_R) are reported in Table 3. As can be seen, in TX-100 and CTAB micellar media, the Φ_R values are barely affected by solvent, while the bleaching is appreciably slowed compared with ethanol. Consequently, based on eqn. (3), the colourability, i.e. the maximum colour intensity attained, increases in these media compared with a homogeneous solution.

The AOT/toluene/water systems were investigated keeping the surfactant concentration constant ($[AOT] = 0.1 \text{ mol dm}^{-3}$) and using different amounts of water ($\omega = [H_2O]/[AOT] = 2, 4, 5, 8$), which changes the aggregation number from 44 ($\omega = 2$) to 112 ($\omega = 8$).¹¹ Therefore, the concentration and micelle size change. The parameters reported in Table 3 correspond to $\omega = 5$. As can be seen from the Table, both Φ_R and k_A values increase compared with direct micelles, the latter parameter is also markedly affected by ω (at 290 K: $k_A = 0.8$, with $\omega = 2$; $k_A = 2.0$, with $\omega = 4$; $k_A = 2.6$, with $\omega = 5$; $k_A = 3.6$, with $\omega = 8$). Consequently, colourability decreases with increasing ω .

In order to test viscosity effects, kinetic measurements were carried out in linear chain alcohols of increasing viscosity. In Table 4, the results (k_A , activation energy, E_a , and frequency factor, k_0) obtained with **1** in homogeneous alcoholic solutions are compared with TX-100. The decay kinetics of **1** in TX-100 at different temperatures and the Arrhenius plot utilised to evaluate E_a are shown in Fig. 4. Since the differences

Table 3 Photokinetic data for **1** and **2** in micellar solutions and in ethanol at 290 K

	TX-100 (3.4 mol dm ⁻³)		CTAB (1.0 mol dm ⁻³)		AOT (0.1 mol dm ⁻³)		EtOH		MCH	
	Φ_R	k_A/s^{-1}	Φ_R	k_A/s^{-1}	Φ_R	k_A/s^{-1}	Φ_R	k_A/s^{-1}	Φ_R	k_A/s^{-1}
1	0.34	0.041	0.20	0.08	0.46	0.84	0.33	0.10	0.41	0.11
2	0.30	0.26	0.21	0.28	0.54	2.6	0.29	1.5	0.49	0.03

detected in the kinetic parameters among the different alcohols are small and randomly spread, they were considered to be meaningless.

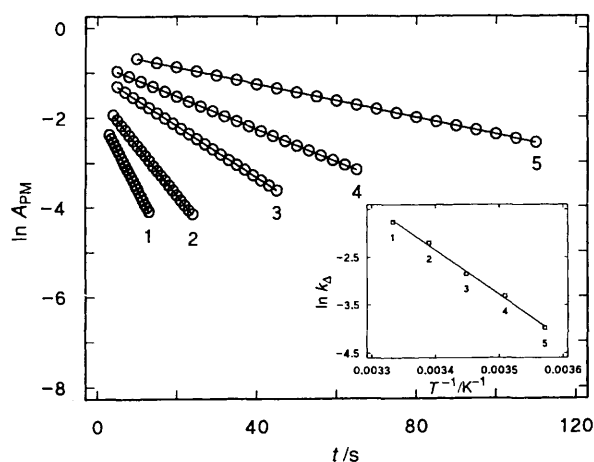
Thermochromism

Non-irradiated micellar solutions of **2** showed an absorption band in the visible region at room temperature, denoting that a thermal equilibrium is established between the closed and open forms, as already observed in ethanol and toluene.⁷ This means that **2** is a thermochromic molecule.

The equilibrium constant, K [eqn. (4)], was calculated from the absorbance in the visible region of the non-irradiated photochrome solution (C_0 represents the total concentration), choosing the ϵ_{PM} values as previously described.

Table 4 Kinetic parameters of the thermal bleaching of **1** in alcohols [methanol (MeOH), *n*-propanol (PrOH), *n*-pentanol (PeOH), *n*-octanol (OtOH)] and TX-100 at 298 K

	$\eta/\text{mPa s}$	k_A/s^{-1}	$E_a/\text{kJ mol}^{-1}$	$k_0/10^{12} \text{ s}^{-1}$
MeOH	0.548	0.33	88	600
PrOH	1.979	0.54	75	5
PeOH	3.566	0.46	79	70
OtOH	7.379	0.34	75	5
TX-100		0.099	79	40

**Fig. 4** First-order kinetics and Arrhenius plot (inset) for the thermal bleaching of **1** in TX-100 at different temperatures: (1) 300, (2) 295, (3) 285, (4) 280, (5) 280 K**Table 5** Equilibrium constant (K) and forward reaction rate constant (k'_A) of **2** in microheterogeneous and homogeneous solutions at 298 K

solvent	$10^2 K$	$k'_A/10^{-2} \text{ s}^{-1}$
CTAB	5.3	3.1
TX-100	1.8	0.97
AOT	0.6	3.2
EtOH	0.8	2.6
toluene	0.5	0.07

$$K = \frac{[\text{PM}]}{[\text{SO}]} = \frac{A_{\text{PM}}/\epsilon_{\text{PM}}}{C_0 - A_{\text{PM}}/\epsilon_{\text{PM}}} \quad (4)$$

The K values in micelle and the kinetic parameters of the forward reaction ($k'_A = Kk_A$) at 298 K are reported in Table 5 along with the values measured in ethanol and toluene. In homogeneous solution, the equilibrium constant increases with solvent polarity.⁷ In microheterogeneous solutions of CTAB and TX-100 the same trend is observed, since the polarity is higher in CTAB than TX-100. The rates of the colour-forming reactions are similar to those for ethanol in TX-100 and CTAB micellar media; therefore, the increase in the K value is determined by the deceleration of the bleaching reaction.

In AOT/toluene/water, thermochromism of **2** was barely detectable at room temperature: the K value is of the same order of magnitude as that determined in toluene.⁸

Discussion

The closed SO form, owing to its non-polar nature, was expected to solubilise in microheterogeneous systems in the less polar microenvironment, *i.e.* in the micellar core for TX-100 and CTAB, and in the bulk hydrocarbon phase for AOT micelles. The open PM form, which consists of a resonance hybrid of a quinoid and a bipolar structure, once formed under UV irradiation, may migrate in a more-polar environment, that is, the micellar surface or bulk water, for normal micelles, and near the polar interface between the water pool and the surfactant heads, for inverted micelles.

The absorption spectra of the closed forms are generally scarcely affected by changing solvent, while those of the open PM forms exhibit positive solvatochromism (bathochromic shift of the absorption band with increasing solvent polarity).⁷ Therefore, the spectral position of the colour band should give a good indication of the polarity of the solubilisation site of PM. The λ_{max} values measured (Table 1) are very close to the values for ethanol in TX-100 for both molecules and somewhat higher than for ethanol in CTAB; those in AOT micellar solution are closer to non-polar solvents. By interpolating these λ_{max} values in a solvatochromic correlation with the $E_T(30)$ solvent-polarity parameter of Dimroth *et al.*,¹⁷ the polarity range of the solubilisation sites can be obtained [$E_T(30)$ values reported in parentheses in Table 1]. By comparing these values, it can be stated that the PMs are solubilised in TX-100 and CTAB in a site near the micellar surface, at a polarity value which is halfway between the bulk water and the micellar inner core. The small, but detectable, red-shifts observed in CTAB *vs.* TX-100 are in agreement with the relatively higher polarity exhibited by the first micellar medium.

The λ_{max} shifts, determined in AOT micellar solutions, indicate that the solubilisation site is essentially non-polar, approximately corresponding to a microenvironment comparable to, or somewhat less polar than, that in toluene. It could be thought that the PMs, solubilised in the hydrocarbon phase, behave in a manner which is independent of the presence of micellar aggregates. In reality, not only the λ_{max} value,

but also the spectral distribution of **1** [Fig. 1(a)] in AOT is halfway between a less-polar (MCH) and a more-polar (CTAB) environment. The change in spectral distribution with changing solvent polarity may be due either to the presence of different conformations,¹⁷ which alter their equilibrium ratio, or to a change in geometry of the ground state relative to the excited state. Bleaching rate measurements carried out at different wavelengths cannot give any indication about the presence of conformers since their equilibration is much faster than deactivation.

Micellar effects on photophysical parameters can be due either to micropolarity or to microviscosity. The increase of the SO fluorescence quantum yield in TX-100 micellar solution relative to ethanol (Table 2) is assigned to increased microviscosity,[†] since the micellar polarity of TX-100 is close to ethanol polarity, as shown by the spectral position of the absorption band. The occupation number effect on Φ_F (which decreases with increasing n) probably indicates the occurrence of bimolecular processes in the micelle which compete with emission.

Viscosity seems not to affect the reaction yield in TX-100 and CTAB. Given the large difference between Φ_R and Φ_F , the increase of the latter in TX-100 cannot lead to detectable effects on Φ_R . Since the microviscosity increase in TX-100 and CTAB micelles, compared with homogeneous systems, it is probably the main reason of the bleaching rate deceleration.

In AOT, the bleaching rate increases, and much more for **2**, where just the opposite was expected based on polarity effects by comparing photokinetic results in EtOH and MCH (Table 3). This is difficult to explain. Tentatively, it can be attributed to the effect of curvature at the micellar interface which increases with decreasing ω . As the curvature increases, the surface pressure is larger, which could force the PM molecules to align at the interface and thus to affect the closing rate.

The TX-100 and CTAB micellar effects on the thermochromism of **2** (Table 5) are in line with the polarity effect, already observed in homogeneous solution,⁷ which favours the establishment of thermo-equilibrium. This explains the K value in the more-polar CTAB micelles which is greater than in TX-100 micelles. In addition, K increases in micellar *vs.* homogeneous systems, because the colour-forming rate is approximately unchanged, while the colour-fading rate decreases in micelles.

In conclusion, the results obtained show that micellar effects on photochromism and thermochromism of spiro[indoline-oxazines], even though not dramatic, denote some interesting behaviour. It has been shown that the SOs can solubilise in an aqueous medium if hydrophobic structures are present. Compared with ethanol, which is the solvent most similar in polarity to the normal micellar

systems (TX-100 and CTAB), the photo- and thermo-colourability increase in the micelle. Both effects depend on the slowing down of the bleaching process for the molecule embedded in the micelle. In AOT inverted micelles, the opposite occurs; both photo- and thermo-chromism are lowered.

Financial support from the Italian Ministero per l'Università e la Ricerca Scientifica e Tecnologica (Consorzio R.C.E., Bologna) and the Italian Consiglio Nazionale delle Ricerche (Progetto Finalizzato Chimica Fine) is gratefully acknowledged.

References

- 1 R. Richert and H. Bässler, *Chem. Phys. Lett.*, 1985, **116**, 302; H. Eckhardt, A. Bose and V. A. Krongauz, *Polymer*, 1987, **28**, 1959.
- 2 J. Sunamoto, K. Iwamoto, Y. Mohri and T. Kominato, *J. Am. Chem. Soc.*, 1982, **104**, 5502.
- 3 E. E. Polymeropoulos and D. Möbius, *Ber. Bunsen-Ges. Phys. Chem.*, 1979, **83**, 1215; M. Morin, R. M. Leblanc and I. Gruda, *Can. J. Chem.*, 1980, **58**, 2038; D. A. Holden, H. Ringsdorf, V. Deblauwe and G. Smets, *J. Phys. Chem.*, 1984, **88**, 716.
- 4 H. Tomioka and T. Itoh, *J. Chem. Soc., Chem. Commun.*, 1991, 532.
- 5 V. Krongauz, J. Kiwi and M. Grätzel, *J. Photochem.*, 1980, **13**, 89; J. Sunamoto, K. Iwamoto, M. Akutagawa, M. Nagase and H. Kondo, *J. Am. Chem. Soc.*, 1982, **104**, 4904.
- 6 A. d'Arco, J. Charmet and M. Cloitre, *Rev. Phys. Appl.*, 1982, **17**, 89.
- 7 G. Favaro, F. Masetti, U. Mazzucato, G. Ottavi, P. Allegrini and V. Malatesta, *J. Chem. Soc., Faraday Trans.*, 1994, **90**, 333.
- 8 G. Favaro, V. Malatesta, U. Mazzucato, G. Ottavi and A. Romani, *J. Photochem. Photobiol. A: Chem.*, 1995, **87**, 235.
- 9 N. Y. C. Chu, *Can. J. Chem.*, 1983, **61**, 300; A. Kellmann, F. Tfibel, R. Dubest, P. Levoir, J. Aubard, E. Pottier and R. Guglielmetti, *J. Photochem. Photobiol. A: Chem.*, 1989, **49**, 63; U. W. Grummt, M. Reichenbacher and R. Paetzold, *Tetrahedron Lett.*, 1981, **22**, 3945; F. Wilkinson, J. Hopley and M. Naftaly, *J. Chem. Soc., Faraday Trans.*, 1992, **88**, 1511.
- 10 K. Kaliasundaram, *Photochemistry in Microheterogeneous Systems*, Academic Press, London, 1987.
- 11 R. A. Day, B. H. Robinson, J. H. R. Clarke and J. V. Doherty, *J. Chem. Soc., Faraday Trans.*, 1979, **75**, 132.
- 12 S. R. Meech and D. Phillips, *J. Photochem.*, 1983, **23**, 193.
- 13 K. Kaliasundaram and J. K. Thomas, *J. Am. Chem. Soc.*, 1977, **99**, 2039; *J. Phys. Chem.*, 1977, **81**, 2176.
- 14 V. Malatesta, M. Milosa, R. Millini, L. Lanzini, P. Bortolus and S. Monti, *Mol. Cryst. Liq. Cryst.*, 1994, **246**, 41; V. Malatesta, L. Montanari and R. Millini, *J. Am. Chem. Soc.*, 1995, **117**, 6258.
- 15 A. Bar and G. Gauglitz, *J. Photochem. Photobiol. A: Chem.*, 1989, **46**, 15; B. Borderie, D. Lavabre, J. C. Micheau and J. P. Laplante, *J. Phys. Chem.*, 1992, **96**, 2953; G. Gauglitz and E. Scheerer, *J. Photochem. Photobiol. A: Chem.*, 1993, **71**, 205.
- 16 G. Favaro, V. Malatesta, U. Mazzucato, C. Miliani and G. Ottavi, *Proc. Ind. Acad. Sci.*, 1995, in the press.
- 17 K. Dimroth, C. Reichardt, T. Siepmann and F. Bohlmann, *Liebigs. Ann. Chem.*, 1963, **661**, 1.
- 18 Shinitzky, *Isr. J. Chem.*, 1974, **12**, 879; N. J. Turro and Y. Tanimoto, *J. Photochem. Photobiol.*, 1981, **34**, 157.

[†] Measured microviscosities are of the order of 15–30 mPa s for normal micelles.¹⁸